Article

Tuning Membrane Thickness Fluctuations in Model Lipid Bilayers

Rana Ashkar,[1,2] Michihiro Nagao,[1,3,*] Paul D. Butler,[1,4] Andrea C. Woodka,[5] Mani K. Sen,[6] and Tadanori Koga[6,7]
[1]National Institute of Standards and Technology (NIST) Center for Neutron Research, National Institute of Standards and Technology, Gaithersburg, Maryland; [2]Department of Material Science and Engineering, University of Maryland, College Park, Maryland; [3]Center for Exploration of Energy and Matter, Indiana University, Bloomington, Indiana; [4]Department of Chemical & Biomolecular Engineering, University of Delaware, Newark, Delaware; [5]Department of Chemistry & Life Science, United States Military Academy, West Point, New York; [6]Department of Materials Science and Engineering and [7]Chemical and Molecular Engineering Program, Stony Brook University, Stony Brook, New York

ABSTRACT Membrane thickness fluctuations have been associated with a variety of critical membrane phenomena, such as cellular exchange, pore formation, and protein binding, which are intimately related to cell functionality and effective pharmaceuticals. Therefore, understanding how these fluctuations are controlled can remarkably impact medical applications involving selective macromolecule binding and efficient cellular drug intake. Interestingly, previous reports on single-component bilayers show almost identical thickness fluctuation patterns for all investigated lipid tail-lengths, with similar temperature-independent membrane thickness fluctuation amplitude in the fluid phase and a rapid suppression of fluctuations upon transition to the gel phase. Presumably, in vivo functions require a tunability of these parameters, suggesting that more complex model systems are necessary. In this study, we explore lipid tail-length mismatch as a regulator for membrane fluctuations. Unilamellar vesicles of an equimolar mixture of dimyristoylphosphatidylcholine and distearoylphosphatidylcholine molecules, with different tail-lengths and melting transition temperatures, are used as a model system for this next level of complexity. Indeed, this binary system exhibits a significant response of membrane dynamics to thermal variations. The system also suggests a decoupling of the amplitude and the relaxation time of the membrane thickness fluctuations, implying a potential for independent control of these two key parameters.

INTRODUCTION

Lipids are the major component of biological membranes through which a delicate balance of nutrients within and outside the cell is maintained. For a long time, this complex functionality in cell membranes was mainly attributed to membrane proteins while lipid bilayers were overlooked as structureless support matrices. Over the last few decades, however, more focus has been directed to the role of lipids in mediating membrane functions (1–3). Conclusions of recent experimental and numerical studies support a growing consensus that lipid bilayers are far from inert and can have an essential role in determining the function of membrane proteins (4,5). The results of such studies clearly show that the behavior of membrane proteins can be severely compromised depending on their structural response to the thickness and curvature of the host bilayer (1,6,7). Unfortunately, much less is known about the dynamical interactions between proteins and lipid membranes despite the recognition that protein functions are ultimately governed by their local dynamics and that protein binding mechanisms are most likely driven by dynamical synergy between the proteins and the bilayer. Based on the energy landscape of membrane proteins, one would expect the synergistic dynamics to not only be important at the longer timescales of microseconds to milliseconds, but also at the much faster picosecond-to-nanosecond timescales. While these are more difficult to experimentally probe, it is becoming increasingly clear that they play a significant role in protein functionality (8), protein-protein binding (9), and enzyme catalysis (10). Indeed, there is growing realization that a number of biological functions, while being directly linked to slow protein dynamics, have their origins in the faster dynamics through solvent interactions (11) or through a dynamical hierarchy in which faster motions control the slower ones (8). However, the full extent of the role of fast dynamics is still poorly understood due to the experimental difficulties in probing this time regime. Interestingly, these timescales coincide with those of collective thermal fluctuations in lipid bilayers (12,13), which starts to suggest that tuning these fluctuations is critical for medical applications requiring selective macromolecule binding. Of particular interest in this context are membrane thickness fluctuations whose dynamics are on the same timescale as conformational transitions in proteins (8) and that have been associated with other membrane functions such as pore formation (14) and passive permeation (15).

Efforts in studying bilayer thickness fluctuations have been hindered by limitations of experimental techniques

Submitted February 18, 2015, and accepted for publication May 28, 2015.
*Correspondence: mnagao@indiana.edu
Editor: Dr. Francesca Marassi.

0006-3495/15/07/0106/7 $2.00
http://dx.doi.org/10.1016/j.bpj.2015.05.033

that can simultaneously access the proper length and timescales. In most cases, the experimental evidence for local membrane fluctuations has been rather indirect (16,17) or inferred from simulations (18,19). More recently, neutron spin-echo (NSE) spectroscopy was effectively used for direct observation of membrane fluctuations in oil-swollen surfactant bilayers (20) and unilamellar lipid vesicles (12). The NSE studies on single-component lipid bilayers with different lipid tail lengths, i.e., DMPC (dimyristoylphosphatidylcholine), DPPC (dipalmitoylphosphatidylcholine), and DSPC (distearoylphosphatidylcholine), revealed some interesting membrane dynamics. Membrane thickness fluctuations were only observable in the fluid phase of the bilayer, implying that such fluctuations are either completely suppressed in the gel phase of the membrane (19) or are slowed down beyond the temporal resolution of the NSE technique. The study also showed almost identical thickness fluctuation patterns (12) in the bilayers, regardless of the length of the lipid molecules used. This invariability in the dynamical behavior relative to lipid tail-length can be attributed to geometrical constraints caused by the minimalistic bilayer composition in this overly simplistic system, which favors uniform bilayer thickness and lateral membrane homogeneity.

However, if the lateral and/or normal symmetry in the membrane is broken, as in biological membranes, one would expect the change in the membrane energetics to drive the system into a more dynamic state. In this study, we investigate the effect of lipid tail-length mismatch in breaking the symmetry and regulating membrane dynamics. We consider as a model system a mixture of length-mismatched DMPC and DSPC molecules characterized by four additional carbon atoms in DSPC tails. The two molecules experience distinct transition temperatures, T_m, at which the tails change from a stiff stretched configuration (gel phase) to a flexible, more coiled configuration (fluid phase). For tail-deuterated (dt) lipids, the transition temperatures are T_m (dtDSPC) = 50.5°C and T_m (dtDMPC) = 20.5°C (12), yielding a broad thermal range of gel-fluid coexistence in DMPC/DSPC mixtures (21,22). Additionally, the two lipid molecules experience dramatic changes in their tail-length mismatch of $\approx$1 nm in the fluid and gel phases and $\approx$2 nm in the gel-fluid coexistence phase (12). These remarkable disparities in the transition temperatures and the tail-length mismatch render DMPC/DSPC mixtures an ideal model for these investigations. The broadest gel-fluid coexistence phase (21) is obtained for an equimolar mixture of DMPC and DSPC, which is the focus of this study. Due to neutron scattering sensitivity to deuterium labeling, we employ selective deuteration to probe different bilayer features. For example, thickness fluctuation parameters are best obtained from tail-contrast-matched vesicles of primarily perdeuterated-tail forms of DMPC and DSPC such that the tail region in the bilayer contrast-matches the carrier solvent (D_2O) (see Table S1 in the Supporting Material). This is the main system used in this work unless otherwise noted.

MATERIALS AND METHODS

Materials

The lipids were purchased from Avanti Polar Lipids (Alabaster, AL) and used without any further purification. The equimolar mixture of DMPC and DSPC was prepared as discussed in Section S1 in the Supporting Material. The lipids were weighed in powder form and dissolved into chloroform for good dissociation, after which the chloroform was evaporated under flow of nitrogen gas. The lipid mixture was then put under vacuum overnight to ensure full evaporation of the chloroform. The dried lipids were then dispersed in D_2O above $T = 55$°C. Unilamellar vesicles were obtained by extruding the mixture, at $T = 60$°C, through polycarbonate filters with pore sizes 400, 200, and 100 nm, consecutively. The extruded solutions were kept above $T = 55$°C until measured.

Methods

Density measurement

To determine the transition temperatures of the mixed lipid bilayers, the solution density was measured using a model No. DMA5000 density meter (Anton Paar, Ashland, VA). Knowing that the lipid molecular density changes dramatically at the gel-fluid transition temperature, temperature-dependent density measurements were conducted over a temperature range from $T = 65$°C to $T = 15$°C with a step of 0.2°C.

Small-angle neutron scattering measurement

Small-angle neutron scattering (SANS) experiments were performed at the NG7-30-meter SANS at the National Institute of Standards and Technology (NIST) (23,24). The selected q range was from 0.03 to 5 nm^{-1} with the use of a 0.6-nm neutron wavelength. The samples used were put in 1-mm-thick quartz cells. The sample temperature was decreased from $T = 65$°C to $T = 15$°C using a circulation bath with an accuracy better than 0.5°C. The raw data were processed via an established reduction protocol to obtain absolute scattering intensity in units of cm^{-1} (25). Data fitting was performed using the software SasView (www.sasview.org).

Small-angle x-ray scattering measurement

Small-angle x-ray scattering (SAXS) measurements were performed at the x27c beam line at Brookhaven National Laboratory (Upton, NY). The accessed q range was 1 to 3.5 nm^{-1} using a wavelength of 0.137 nm at a sample-to-detector distance of 95.7 cm. The scattered photons were collected by a charge-coupled device camera. The detector distance and q value were calibrated using silver behenate. The samples were measured in a 1-mm-diameter capillary tube taped to a temperature-controlled stage. The measurements were done over a temperature range of 65–25°C with an accuracy of $\pm$1°C. Data reduction, including background subtraction, was performed using the xPOLAR software developed at Precision Works NY, Inc. (East Setauket, NY).

NSE measurement

NSE experiments were performed using the NG5-NSE spectrometer at NIST (26) at neutron wavelengths of 0.6 and 0.8 nm with a wavelength spread of ~18%. The measured q ranges spanned from 0.4 to 1.8 nm^{-1} and Fourier times, t, from 0.05 to 40 ns. The tail-contrast-matched sample was measured in a 4-mm-thick cell and the hydrogenated sample in a 1-mm-thick cell. The temperature was varied from $T = 65$°C to $T = 15$°C using a circulating bath with an accuracy better than $\pm$0.1°C. The obtained NSE signals were reduced to the intermediate scattering function using the software DAVE (27), which properly accounts for background and resolution corrections.

RESULTS AND DISCUSSION

Due to strong coupling between the gel-fluid transition and membrane structure and dynamics (12), a precise determination of the phase boundaries was made. Temperature-controlled density measurements on the equimolar tail-contrast-matched vesicles show an upper and a lower transition temperature, $T_u \approx 41°C$ and $T_l \approx 27.5°C$, as defined from the two maxima in the density gradient (Fig. 1). The analogous fully hydrogenated-lipid sample shows a similar trend with an upward shift of 2.7°C in the transition temperatures, in accord with literature values (see Table S1). In contrast with the sharp transition observed in single-lipid bilayers (12), the density in the binary system shows gradual changes around the phase boundaries. This behavior, along with the shifts in the transition temperatures (*phase transition bars* in Fig. 1), is attributed to a thermal delay in the collective gel-fluid transition of individual species induced by lateral rearrangements of lipid molecules (22,28).

The dynamical response of the bilayer in the different phases of Fig. 1 is measured using neutron spin echo (see Fig. S1 in the Supporting Material). The NSE measurements directly yield the decay rate, Γ, of the dynamics probed at well-defined length scales determined by the wavevector transfer, q. The q-dependence of the decay rate depends on the nature of the membrane dynamics as shown in Fig. S2. If the membrane only experiences bending fluctuations, the decay rates should exhibit a simple q^3 dependence, as shown by Zilman and Granek (29). However, the measured decay rates of the tail-contrast-matched bilayers (Fig. 2) show a remarkable deviation from such a q^3 behavior at $q \approx 1\ \mathrm{nm}^{-1}$. More precisely, the q values at which the thickness fluctuations are most prominent correspond to the membrane thickness at that temperature, as shown in Fig. S3. Previous reports on similar systems have attributed this enhancement to thickness fluctuations

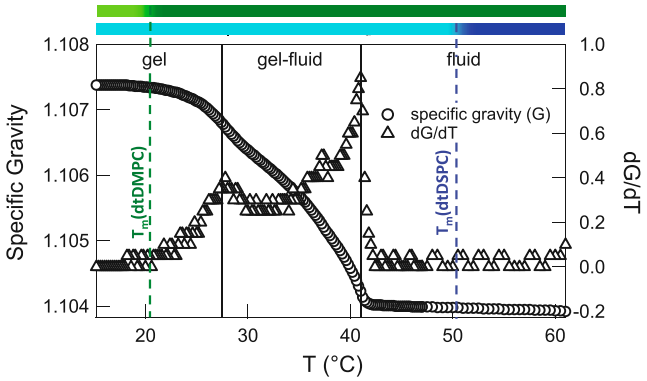

FIGURE 1 Temperature dependence of specific gravity and its gradient for the tail-contrast-matched equimolar DMPC/DSPC mixture. (*Solid vertical lines*) Upper and lower phase boundaries. (*Phase transition bars*) Gel (*light*) or fluid (*dark*) state of single-component DMPC (*upper bar*) and DSPC (*lower bar*) bilayers, as determined from the melting temperatures of the two lipids (*dashed lines*). To see this figure in color, go online.

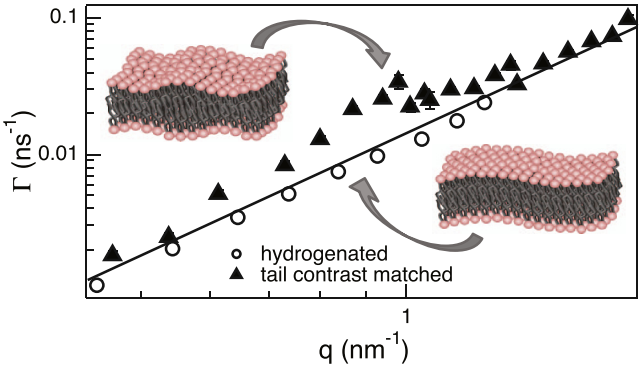

FIGURE 2 The q dependence of Γ for hydrogenated and tail-contrast-matched samples at $T = 65°C$. (*Solid line*) The q^3 behavior of bending fluctuations is represented by the first term in Eq. 1. The enhancement in the decay rates of the tail-contrast-matched sample corresponds to membrane thickness fluctuations. Error bars represent ±1 SD in the entire article and are smaller than the symbol size in this figure. To see this figure in color, go online.

(12) and showed that the dynamics in such systems can be described by a linear combination of bending and thickness fluctuation contributions (12,20) such that

$$\Gamma = 0.0058\frac{k_BT}{\eta_{D_2O}}\sqrt{\frac{k_BT}{\kappa}}q^3 + \frac{\left(\tau_{TF}q_0^3\right)^{-1}}{1+\left(q-q_0\right)^2\xi^2}q^3, \quad (1)$$

where k_BT is the thermal energy, η_{D_2O} is the viscosity of D_2O, κ is the bending modulus, τ_{TF} is the relaxation time of thickness fluctuations, q_0 is the peak position of Γ/q^3, and $1/\xi$ is the half-width at half-maximum of the Lorentz fit function. The first term captures noninteracting membrane bending fluctuations proposed by Zilman and Granek (29) including the refinement by Watson and Brown (30) and Lee et al. (31). The second term is an empirical expression for thickness fluctuations (12,20,32).

For fully hydrogenated bilayers, due to the much lower contrast between the headgroups and the tail region, the enhancement occurs at much higher q values and is outside the q range of the measurement. This is clearly reflected in the simple q^3 dependence of the decay rate for the hydrogenated bilayers (Fig. 2), whose dynamics are dominated by membrane bending fluctuations over the accessed q range. Because both hydrogenated and tail-contrast-matched bilayers exhibit the same bending fluctuation behavior, as manifested by the identical q^3 component of their decay rates (Fig. 2), the most reliable determination of the bending properties is obtained from the data on the hydrogenated bilayers.

The bending modulus κ, found from the fits of the first term in Eq. 1 to the decay rates, exhibits a gradual change at the transition temperatures as shown in Fig. 3, in contrast with the sharp transition reported in single-component bilayers (12,33). At high T, both binary and single-lipid bilayers have the same asymptotic value of the bending modulus $\kappa \approx 20\ k_BT$. More pronounced differences, however, are

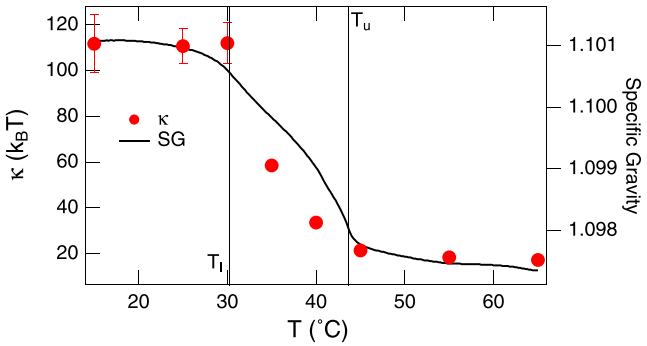

FIGURE 3 Temperature dependence of κ on the hydrogenated DMPC/DSPC vesicles. (*Vertical lines*) Transition temperatures T_u and T_l; (*solid line*) measured specific gravity. To see this figure in color, go online.

observed in the gel-fluid coexistence region and at low temperatures. We attribute these discrepancies to the lateral phase separation of the DMPC and DSPC molecules into domains with different stiffness coefficients. For instance, in the gel-fluid coexistence region, the fluid DMPC domains are expected to maintain a certain level of flexibility in the membrane despite the presence of stiff DSPC gel domains. The strong correlation between the bending modulus and the membrane density as shown in Fig. 3 corroborates this conclusion and suggests that the average lateral membrane compressibility (directly related to κ (34,35)) is controlled by the bilayer density.

Fits of the second term of Eq. 1 to the decay rates on the tail-contrast-matched vesicles yield the two parameters, τ_{TF} and ξ, that describe thickness fluctuations. Fig. 4 shows the thermal dependence of the relaxation time, τ_{TF}, of thickness fluctuations in the binary membranes along with the previously estimated τ_{TF} values for the DMPC and DSPC bilayers (12). In the fluid phase, i.e., above $T = 45°C$, $\tau_{TF} \approx$ 100 ns and is comparable to the relaxation times observed in the single-lipid bilayers (12). In the gel-fluid coexistence region, however, thickness fluctuations experience a remarkable slowdown, in agreement with our previous suggestion (12) that the thickness fluctuations in single-component bilayers may not be totally suppressed below the main transition temperature but are slowed down beyond the temporal resolution of NSE.

An estimate of the fluctuation amplitude for tail-contrast-matched vesicles can be extracted from ξ using the following expression, $d_m\xi^{-1}/q_0$, as discussed in Nagao et al. (32). Unlike the fluctuations in single-lipid bilayers (12), which lack any temperature dependence above T_m, the equimolar mixture shows strong enhancement of the fluctuation amplitude at high-T (Fig. 5). In fact, at temperatures $>>T_u$, the thickness fluctuation amplitude in equimolar vesicles is ~2–3 times that observed in the single-component vesicles (12). We should note that the average radius of the vesicles and the vesicle concentration are almost identical in all the samples studied so far, which rules out membrane curvature and intervesicle interaction as the source of the observed differences.

To better understand the thickness fluctuation behavior, we examine the temperature dependence of the membrane thickness. The bilayer thickness, extracted from SANS and SAXS data, fits to a three-shell vesicle model (36) (see Fig. S4), is shown in Fig. 6 over a wide thermal range. In the absence of compression, extension, or interdigitation, conservation of volume arguments require the average membrane thickness to be the mean value of the thicknesses of the pure component bilayers. We model the thickness of DMPC and DSPC bilayers by an error-function (sigmoidal distribution) that is centered at the corresponding transition temperature (as defined from density measurements) and which approaches the thickness of the gel (fluid) membrane below (above) the transition. The values for gel and fluid

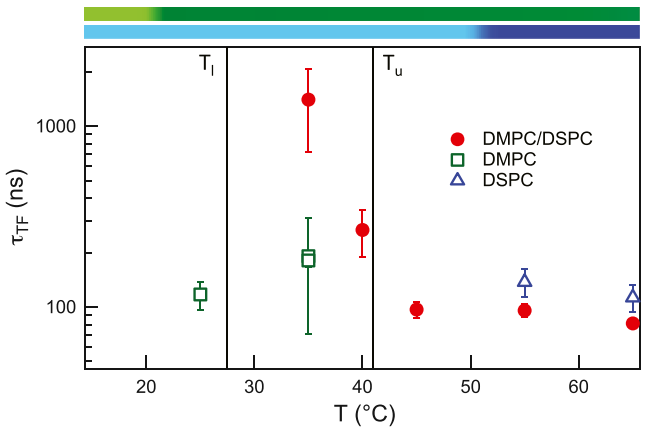

FIGURE 4 Thermal dependence of the relaxation time of thickness fluctuations in single-component DMPC and DSPC bilayers and the equimolar DMPC/DSPC mixture. (*Vertical lines*) T_u and T_l; (*phase transition bars*) are the same as in Fig. 1. To see this figure in color, go online.

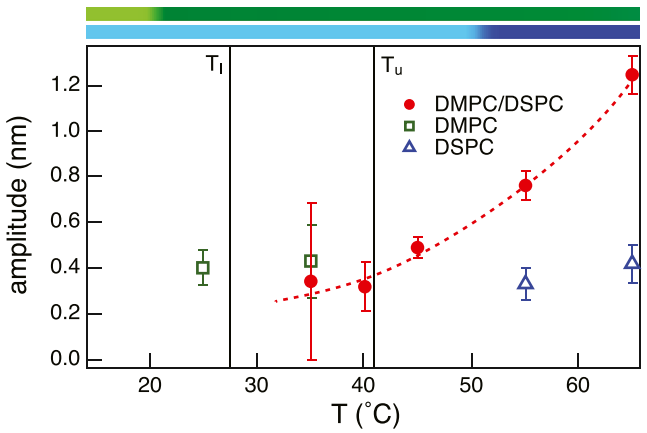

FIGURE 5 Thermal behavior of thickness fluctuation amplitudes for DMPC and DSPC bilayers and their equimolar mixture. (*Vertical lines* and *phase transition bars*) Gel and fluid transitions in the mixed and pure systems, respectively, as described in Fig. 1. To see this figure in color, go online.

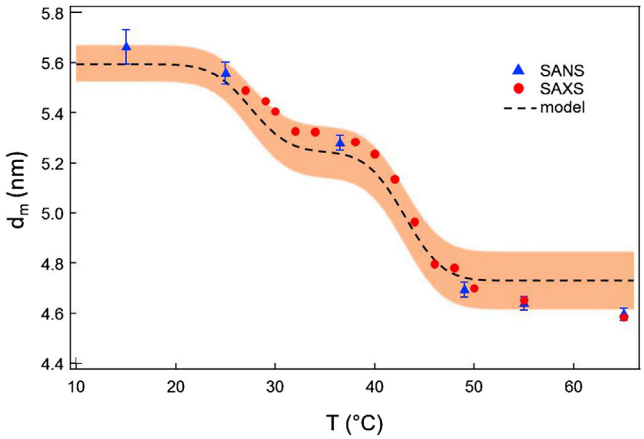

FIGURE 6 Temperature dependence of the thickness of equimolar DMPC/DSPC bilayers as obtained from SANS and SAXS data. (*Dashed line*) Based on the model described in the text; (*shaded area*) margin of error. To see this figure in color, go online.

DMPC and DSPC membrane thickness, obtained from SANS data on single-component vesicles using the same fitting routine, are d_m (DMPC) = (5.0 ± 0.1) nm and d_m (DSPC) = (6.2 ± 0.1) nm in the gel phase and d_m (DMPC) = (4.3 ± 0.1) nm and d_m (DSPC) = (5.1 ± 0.1) nm in the fluid phase, in agreement with previous reports on these systems (37). From these values we then model the thickness of the DMPC/DSPC bilayers as the mean of the two sigmoidal distributions (*dashed line* in Fig. 6). The SANS/SAXS fit values of the binary membrane thickness nicely follow the three-plateau pattern, which naturally results from the hypotheses of sigmoidal distribution discussed earlier. Thus, in the high temperature region, where both DMPC and DSPC lipids are expected to be fully fluid and relatively well mixed (22,28), both must experience a nonoptimal tail packing geometry. The resulting additional entropic stretching/shrinking motions of the lipid molecules could then manifest in fluctuations normal to the bilayer surface, leading to larger thickness fluctuation amplitudes. More insight into the energetics behind this behavior can be obtained from deformation free energy calculations (38) in which such motions are generally captured by a compression-expansion energy term. Such calculations on this equimolar mixture, in the fluid phase, show an increase in the membrane compressibility compared to the single-component analogs (M. Nagao and R. Ashkar, unpublished). This increase in membrane compressibility would naturally result in an enhancement in the fluctuation amplitude observed here (Fig. 5), in accord with previous findings on similar systems (39).

As the temperature decreases toward T_u, the membrane experiences a damping in the thickness fluctuations as manifested by the gradual decrease in the fluctuation amplitude (Fig. 5). It is important to point out that in the thermal region between T_u and T_m (DSPC), DSPC molecules are below their melting transition temperature. In this region, we conjecture the possible existence of small transient DSPC clusters that reduce the area of fluid domains that can support enhanced thickness fluctuations, and may even anchor the surrounding molecules, limiting their extensions or compressions and consequently lowering the average amplitude of the membrane thickness fluctuations. Such clusters have been reported in contrast-matched SANS experiments near the upper gel-fluid transition of the mixture (22) and in Monte Carlo simulations on fluid DMPC/DSPC bilayers (21).

In the gel-fluid coexistence region, the thickness fluctuation amplitude of equimolar DMPC/DSPC membranes becomes comparable to that of the single-component bilayers, which agrees with our previous hypothesis (12) that the thickness fluctuation amplitude is determined by geometrical constraints. Indeed, in this region we expect the two lipids to be mostly segregated into DSPC gel domains and DMPC fluid domains (40,41). From our previous results, we expect only the fluid DMPC domain fluctuations to be measurable and their amplitude to be ≈0.4 nm, which matches the amplitude measured in this coexistence region within the experimental error. On the other hand, we would expect the growth of the DSPC gel domains in this region to force a cutoff on the longer wavelength modes of the thickness fluctuations. Clearly this is not impacting the amplitude within our experimental resolution, suggesting that either the size of the domains are larger than the lateral extent of the fluctuations, or that the amplitude is not affected by the contribution from longer wavelengths. We would also expect a reasonable interfacial region between the domains with significantly altered tail states. If one postulates that the fluctuations are only slowed down and not suppressed in the gel phase (12), this interfacial region, somewhere between the gel and fluid states, could easily lead to the measurable slowdown in thickness fluctuations. In this case, the data suggest the amplitudes remain the same in the gel phase, in agreement once again with the concept of geometric constraints.

To summarize, this work utilizes NSE to access unique collective membrane dynamics in binary lipid bilayers of equimolar DMPC/DSPC mixtures, along with SANS and SAXS studies for complementary structural characterization. The main findings are briefly listed below.

1) The phase boundaries of the mixture, determined by density measurements, indicate a shift in the transition temperatures, T_u and T_l, relative to the pure components and show a broad thermal range of gel-fluid coexistence phase, in agreement with previous studies.
2) In the high temperature fluid phase ($T >> T_u$), the system shows a dramatic enhancement in the thickness fluctuation amplitude (while maintaining the same relaxation times as in the single-component analogs).
3) As the temperature decreases toward the upper transition temperature, T_u, the thickness fluctuation amplitude decreases to its previously reported value in single component bilayers.

4) In the gel-fluid coexistence region ($T_1 < T < T_u$), a significant increase in the relaxation time of the membrane thickness fluctuations is observed with decreasing temperature.

CONCLUSIONS

We demonstrate that the simple addition of a second lipid component to a lipid bilayer system can introduce the tunability requisite for biological function. The membrane heterogeneity, caused by lipid tail-length mismatch in this minimalistic two-component system, allows us to begin probing the molecular and mesoscale origins of membrane dynamics that is so important to real-world function and materials engineering. Indeed, while tail lengths in single-component systems do not have any noticeable effect on thickness fluctuation parameters, an equimolar mixture of length-mismatched lipids is more responsive to thermal variations over a wide range of temperature. Among the rich dynamics in this DMPC/DSPC mixture, the most intriguing is the dramatic amplification of the thickness fluctuation amplitude in the fluid state, which is of significant relevance to critical membrane phenomena such as budding (42) and pore formation (35,43). The decrease of the fluctuation amplitude to previously reported values as the temperature is lowered from T_m (DSPC) to T_u is attributed to transient DSPC clusters that are expected to form below the main transition of DSPC. In this picture, the size of such clusters is anticipated to be on the nanoscale due to the surrounding molten lipids. Such clusters are reminiscent of the raftlike domains observed in simulations on a similar binary system (44). It is important to point out that the domains formed in the coexistence region do not fall under the same description.

The other striking feature in our results is the decoupling in the thermal response of the amplitude and the relaxation time of thickness fluctuations. While the amplitude exhibits a strong temperature dependence in the fluid phase, the relaxation time is almost constant in this temperature range. The pattern is reversed in the gel-fluid phase of the membrane. Such a decoupling would imply the possibility of independent control of the time and space components of thickness fluctuations, which would be extremely valuable in tuning membrane fluctuations, whether for regulating biological function or delivering therapeutic agents.

We hope that this direct and clear evidence of the unique thermal response of thickness fluctuations in binary lipid membranes will encourage more simulations and experiments targeted toward understanding collective dynamics in multicomponent soft membranes with varying degrees of complexity. At the next level of complexity one might ask how the local equilibrium dynamics couple to longer length and timescale dynamics. In fact, in that context, an intriguing question would be what the response of the dynamics on one length scale would be to a rapid perturbation, say from an external stimuli, on the dynamics at the other length scale. One could in fact envisage the creation of a feedback loop that could provide either an avenue to buffering harmful effects or, conversely, could lead to catastrophic consequences. We believe that using these minimalistic systems, coupling simulation to experiment, and using the NSE technique offer an exciting opportunity to begin carefully and systematically probing these important dynamic phenomena that govern the activity of biological membranes.

SUPPORTING MATERIAL

Supporting Materials and Methods, four figures, and one table are available at http://www.biophysj.org/biophysj/supplemental/S0006-3495(15)00545-7.

AUTHOR CONTRIBUTIONS

R.A. performed SANS and SAXS experiments, analyzed the data, and wrote the article. M.N. designed the research, performed SANS, SAXS, and NSE experiments, analyzed the data, and wrote the article. P.D.B. performed SANS experiments, analyzed the data, and wrote the article. A.C.W. performed NSE experiments and analyzed the data. M.K.S. and T.K. performed SAXS experiments and the data analysis.

ACKNOWLEDGMENTS

R.A., M.N., and P.D.B. thank Professor Peter Olmsted and Dr. John Williamson for valuable discussions and Dr. Elizabeth Kelley for careful reading of the manuscript.

M.N. acknowledges funding support of cooperative agreement No. 70NANB10H255 from National Institute of Standards and Technology (NIST), U.S. Department of Commerce. The authors acknowledge the use of the NIST Center for Neutron Research facilities, which are supported in part by the National Science Foundation under agreement No. DMR-0944772. Use of the National Synchrotron Light Source was supported by the U.S. Department of Energy, Office of Science, Office of Basic Energy Sciences, under contract No. DE-AC02-98CH10886.

Certain commercial equipment, suppliers, or materials are identified in this article to foster understanding. Such identification does not imply recommendation or endorsement by the National Institute of Standards and Technology, nor does it imply that the materials or equipment identified are necessarily the best available for the purpose.

SUPPORTING CITATIONS

Reference (45) appears in the Supporting Material.

REFERENCES

1. Phillips, R., T. Ursell, …, P. Sens. 2009. Emerging roles for lipids in shaping membrane-protein function. *Nature.* 459:379–385.

2. Andersen, O. S., and R. E. Koeppe, 2nd. 2007. Bilayer thickness and membrane protein function: an energetic perspective. *Annu. Rev. Biophys. Biomol. Struct.* 36:107–130.

3. Sachs, J. N., and D. M. Engelman. 2006. Introduction to the membrane protein reviews: the interplay of structure, dynamics, and environment in membrane protein function. *Annu. Rev. Biochem.* 75:707–712.

4. Lingwood, D., and K. Simons. 2010. Lipid rafts as a membrane-organizing principle. *Science.* 327:46–50.

5. Simons, K., and E. Ikonen. 1997. Functional rafts in cell membranes. *Nature.* 387:569–572.
6. Jensen, M. Ø., and O. G. Mouritsen. 2004. Lipids do influence protein function—the hydrophobic matching hypothesis revisited. *Biochem. Biophys. Acta.* 1666:205–226.
7. Perozo, E., D. M. Cortes, …, B. Martinac. 2002. Open channel structure of MscL and the gating mechanism of mechanosensitive channels. *Nature.* 418:942–948.
8. Henzler-Wildman, K., and D. Kern. 2007. Dynamic personalities of proteins. *Nature.* 450:964–972.
9. Lange, O. F., N. A. Lakomek, …, B. L. de Groot. 2008. Recognition dynamics up to microseconds revealed from an RDC-derived ubiquitin ensemble in solution. *Science.* 320:1471–1475.
10. Eisenmesser, E. Z., O. Millet, …, D. Kern. 2005. Intrinsic dynamics of an enzyme underlies catalysis. *Nature.* 438:117–121.
11. Frauenfelder, H., G. Chen, …, R. D. Young. 2009. A unified model of protein dynamics. *Proc. Natl. Acad. Sci. USA.* 106:5129–5134.
12. Woodka, A. C., P. D. Butler, …, M. Nagao. 2012. Lipid bilayers and membrane dynamics: insight into thickness fluctuations. *Phys. Rev. Lett.* 109:058102.
13. Rheinstädter, M. C., J. Das, …, I. Kosztin. 2008. Motional coherence in fluid phospholipid membranes. *Phys. Rev. Lett.* 101:248106.
14. Bennett, W. F., N. Sapay, and D. P. Tieleman. 2014. Atomistic simulations of pore formation and closure in lipid bilayers. *Biophys. J.* 106:210–219.
15. Orsi, M., and J. W. Essex. 2010. Permeability of drugs and hormones through a lipid bilayer: insights from dual-resolution molecular dynamics. *Soft Matter.* 6:3797–3808.
16. Pralle, A., P. Keller, …, J. K. Hörber. 2000. Sphingolipid-cholesterol rafts diffuse as small entities in the plasma membrane of mammalian cells. *J. Cell Biol.* 148:997–1008.
17. Honerkamp-Smith, A. R., S. L. Veatch, and S. L. Keller. 2009. An introduction to critical points for biophysicists; observations of compositional heterogeneity in lipid membranes. *Biochim. Biophys. Acta.* 1788:53–63.
18. Lindahl, E., and O. Edholm. 2000. Mesoscopic undulations and thickness fluctuations in lipid bilayers from molecular dynamics simulations. *Biophys. J.* 79:426–433.
19. West, B., and F. Schmid. 2010. Fluctuations and elastic properties of lipid membranes in the gel $L_{\beta'}$ state: a coarse-grained Monte Carlo study. *Soft Matter.* 6:1275–1280.
20. Nagao, M. 2009. Observation of local thickness fluctuations in surfactant membranes using neutron spin echo. *Phys. Rev. E Stat. Nonlin. Soft Matter Phys.* 80:031606.
21. Michonova-Alexova, E. I., and I. P. Sugár. 2002. Component and state separation in DMPC/DSPC lipid bilayers: a Monte Carlo simulation study. *Biophys. J.* 83:1820–1833.
22. Knoll, W., K. Ibel, and E. Sackmann. 1981. Small-angle neutron scattering study of lipid phase diagrams by the contrast variation method. *Biochemistry.* 20:6379–6383.
23. Glinka, C. J., J. G. Barker, …, W. J. Orts. 1998. The 30 m small-angle neutron scattering instruments at the National Institute of Standards and Technology. *J. Appl. Cryst.* 31:430–445.
24. Choi, S.-M., J. G. Barker, …, P. L. Gammel. 2000. Focusing cold neutrons with multiple biconcave lenses for small-angle neutron scattering. *J. Appl. Cryst.* 33:793–796.
25. Kline, S. 2006. Reduction and analysis of SANS and USANS data using IGOR PRO. *J. Appl. Cryst.* 39:895–900.
26. Rosov, N., S. Rathgeber, and M. Monkenbusch. 2000. Scattering from polymers: characterization by x-rays, neutrons, and light. *ACS Symposium Series*. Oxford University Press, New York, pp. 103–116.
27. Azuah, R. T., L. R. Kneller, …, R. M. Dimeo. 2009. DAVE: a comprehensive software suite for the reduction, visualization, and analysis of low energy neutron spectroscopic data. *J. Res. Natl. Inst. Stand. Technol.* 114:341–358.
28. Bagatolli, L. A., and E. Gratton. 2000. A correlation between lipid domain shape and binary phospholipid mixture composition in free standing bilayers: A two-photon fluorescence microscopy study. *Biophys. J.* 79:434–447.
29. Zilman, A. G., and R. Granek. 1996. Undulations and dynamic structure factor of membranes. *Phys. Rev. Lett.* 77:4788–4791.
30. Watson, M. C., and F. L. H. Brown. 2010. Interpreting membrane scattering experiments at the mesoscale: the contribution of dissipation within the bilayer. *Biophys. J.* 98:L9–L11.
31. Lee, J.-H., S.-M. Choi, …, S. R. Kline. 2010. Thermal fluctuation and elasticity of lipid vesicles interacting with pore-forming peptides. *Phys. Rev. Lett.* 105:038101.
32. Nagao, M., S. Chawang, and T. Hawa. 2011. Interlayer distance dependence of thickness fluctuations in a swollen lamellar phase. *Soft Matter.* 7:6598–6605.
33. Yi, Z., M. Nagao, and D. P. Bossev. 2009. Bending elasticity of saturated and monounsaturated phospholipid membranes studied by the neutron spin echo technique. *J. Phys. Condens. Matter.* 21:155104.
34. Rawicz, W., K. C. Olbrich, …, E. Evans. 2000. Effect of chain length and unsaturation on elasticity of lipid bilayers. *Biophys. J.* 79:328–339.
35. Popescu, D., S. Ion, …, L. Movileanu. 2003. Elastic properties of bilayer lipid membranes and pore formation. *In* Planar Lipid Bilayers (BLMs) and Their Applications. H. T. Tien and A. Ottova, editors. Elsevier Science Publisher, Amsterdam, The Netherlands.
36. Guinier, A., and G. Fount. 1955. Small-Angle Scattering of X-Rays. John Wiley, New York.
37. Lewis, B. A., and D. M. Engelman. 1983. Lipid bilayer thickness varies linearly with acyl chain length in fluid phosphatidylcholine vesicles. *J. Mol. Biol.* 166:211–217.
38. Huang, H. W. 1986. Deformation free energy of bilayer membrane and its effect on gramicidin channel lifetime. *Biophys. J.* 50:1061–1070.
39. Hladky, S. B., and D. W. Gruen. 1982. Thickness fluctuations in black lipid membranes. *Biophys. J.* 38:251–258.
40. Sankaram, M. B., D. Marsh, and T. E. Thompson. 1992. Determination of fluid and gel domain sizes in two-component, two-phase lipid bilayers. An electron spin resonance spin label study. *Biophys. J.* 63: 340–349.
41. Fahsel, S., E.-M. Pospiech, …, R. Winter. 2002. Modulation of concentration fluctuations in phase-separated lipid membranes by polypeptide insertion. *Biophys. J.* 83:334–344.
42. Baumgart, T., S. T. Hess, and W. W. Webb. 2003. Imaging coexisting fluid domains in biomembrane models coupling curvature and line tension. *Nature.* 425:821–824.
43. Movileanu, L., D. Popescu, …, A. I. Popescu. 2006. Transbilayer pores induced by thickness fluctuations. *Bull. Math. Biol.* 68:1231–1255.
44. Meinhardt, S., R. L. C. Vink, and F. Schmid. 2013. Monolayer curvature stabilizes nanoscale raft domains in mixed lipid bilayers. *Proc. Natl. Acad. Sci. USA.* 110:4476–4481.
45. Nallet, F., R. Laversanne, and D. Roux. 1993. Modelling x-ray or neutron scattering spectra of lyotropic lamellar phases: interplay between form and structure factors. *J. Phys. II.* 3:487–502.

"Tuning membrane thickness fluctuations in model lipid bilayers"

Rana Ashkar[1,2], Michihiro Nagao[1,3] Paul D. Butler[1,4], Andrea C. Woodka[5], Mani Kuntal Sen[6], and Tadanori Koga[6,7]

[1] *Center for Neutron Research, National Institute of Standards and Technology, Gaithersburg, MD 20899-6102, USA*

[2] *Department of Material Science and Engineering, University of Maryland, College Park, MD 20742, USA*

[3] *Center for Exploration of Energy and Matter, Indiana University, Bloomington, IN 47408, USA*

[4] *Department of Chemical & Biomolecular Engineering, University of Delaware, Newark, DE 19716, USA*

[5] *Department of Chemistry & Life Science, United States Military Academy, West Point, NY 10996-1905, USA*

[6] *Department of Materials Science and Engineering, Stony Brook University, Stony Brook, NY 11794-2275, USA*

[7] *Chemical and Molecular Engineering program, Stony Brook University, Stony Brook, NY 11794-2275, USA*

S1. Characterization of the membrane phase transitions

Shifts in the transition temperatures are expected in lipids with deuterium labeling, depending on the deuteration level and the amount of the deuterated lipids in the sample. Previous temperature-dependent density measurements on single component DMPC and DSPC lipid bilayers showed significant shifts in the melting temperatures of tail-deuterated (dt) DMPC and DSPC lipids relative to their hydrogenated analogues (1). The reported temperatures for the different lipids are: T_m (DSPC) = 55 °C and T_m (DMPC) = 23 °C for the hydrogenated samples, and T_m (dtDMPC) = 20.5 ˚C and T_m (dtDSPC) = 50.5 ˚C. For the DMPC/DSPC mixtures in this study, the deuterium content in the samples depends on the mixing ratio of the two lipids and the deuteration requirements of the neutron scattering experiments. In this work, we investigate two samples of equimolar DMPC/DSPC bilayers with different neutron scattering contrasts: 1) fully hydrogenated bilayers in D_2O and 2) bilayers with the tail region contrast matched to D_2O. To account for deuteration effects, we use temperature-dependent densitometry to determine the phase boundaries of the two samples. The detailed composition of the two samples and their transition temperatures are reported in Table S1.

Table S1: Compositional (mass) description of the fully-hydrogenated and tail-contrast-matched vesicles of equimolar DMPC/DSPC mixtures used in this study, along with their lower and upper transition temperatures, T_l and T_u respectively, as obtained from density measurements. The mixtures were suspended in the required amount of D_2O at a lipid mass fraction of 10 mg/mL and 100 mg/mL for SANS and NSE measurements, respectively.

	dtDMPC	hDMPC	dtDSPC	hDSPC	T_l	T_u
Fully-hydrogenated	0 mg	9.240 mg	0 mg	10.765 mg	30.2 °C	43.6 °C
Tail-contrast-matched	8.301 mg	0.899 mg	9.677 mg	1.121 mg	27.5 °C	41 °C

S2. Neutron Spin Echo (NSE)

The NSE technique accesses the normalized intermediate scattering function $I(q,t)/I(q,0)$, which for the present system can be fitted to a stretched exponential of the form $\exp[-(\Gamma t)^{2/3}]$ where Γ is the decay rate

and t is the Fourier time (2). An example of the fits to the data collected on the tail-contrast-matched vesicles is shown in Fig. S1 for T = 65 °C. The decay rates are adequately described by a sum of the Zilman-Granek model (2) of bending fluctuations, including the refinement by Watson and Brown (3) and Lee *et al*. (4), and a thickness fluctuation term proposed by Nagao (1, 5, 6). The full expression used for modeling the membrane fluctuations is given by eq. 1 in the main text.

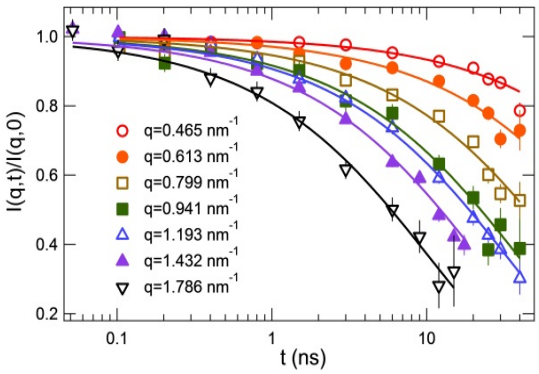

Fig. S1. Normalized intermediate scattering function, $I(q,t)/I(q,0)$, obtained from NSE measurements on the tail-contrast-matched sample at T = 65 °C. The solid lines are fits to the stretched exponential model.

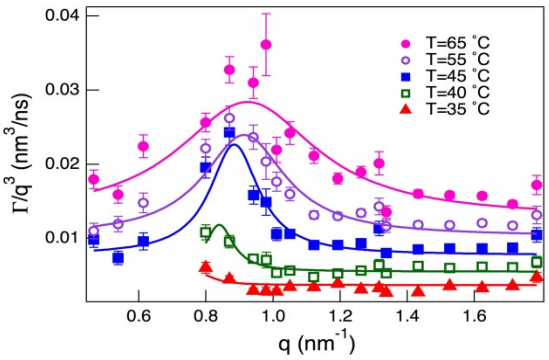

Fig. S2. Temperature variation of the q dependence of Γ/q^3 from the tail-contrast-matched sample. The lines are best fits to the data using eq. 1 in the main text with q_0 values obtained from the dip position in the corresponding SANS data. The shift of the peak position toward lower q with decreasing temperature indicates an increase in the membrane thickness as the mixture transitions into the coexistence phase.

The thickness fluctuation term accounts for the enhancement of the decay rates caused by membrane thickness fluctuations as shown in Fig. S2. The maximum enhancement is observed at q-values that coincide with the dip position in the corresponding SANS scattering pattern (see Fig. S3). The dip position in the SANS signal corresponds to the membrane thickness and can be calculated from a lamellar form factor (7) as $q_0 = \pi / \left(d_m - d_h \right)$ where d_m and d_h are the total membrane thickness and the lipid headgroup thickness, respectively. On the other hand, similar form factor calculations on a fully hydrogenated bilayer (that lacks contrast between head and tail groups) show that the peak position, q_0, in this case occurs at $2\pi/d_m$; *i.e.* q_0 ~ twice the value for the tail-contrast matched bilayers. This value is outside the measurement window of the NSE experiment. Consequently, thickness-fluctuation enhancement of the decay rates of the hydrogenated bilayers cannot be observed over the accessed q-range, as evident from the data shown in Fig. 2 in the main text.

S3. Structural characterization of the lipid bilayers

The response of the structural parameters of the vesicles to the phase transitions was studied by small-angle neutron and x-ray scattering (SANS and SAXS) over a wide temperature range. Fig. S4 shows SANS profiles of tail-contrast-matched unilamellar vesicles at three select temperatures in each of the regions in Fig. 1 in the main article. The data show a dip around q = 1 nm^{-1} which further shifts toward lower q with decreasing temperature, indicating an increase in the bilayer thickness as the lipid

components transition into their gel phase. The solid lines are least-mean square fits to the data using a scattering model for a three-shell vesicle (8). The model takes into account the contrast variations of the head and tail groups of the lipid molecules within the vesicle. Accordingly, the vesicle model is divided into three layers or shells such that the innermost and outermost shells account for the headgroup regions of the inner and outer leaflets, respectively, and the intermediate shell depicts the overall lipid-tail region in both leaflets. Each shell is described by a given thickness and scattering contrast, which are obtained from fits to the scattering data. The same model is used for fitting the SAXS data with careful substitution of the neutron scattering length density by the electron density of the corresponding shell. The membrane thickness, obtained from SANS and SAXS data at various temperatures, is shown in Fig. 6 in the main manuscript.

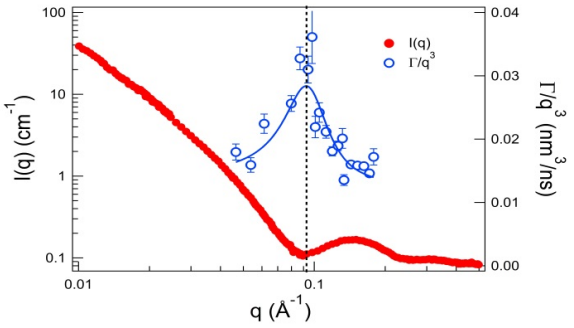

Fig. S3. Overplot of NSE and SANS data on the tail-contrast matched equimolar DMPC/DSPC vesicles at T = 65 °C. The thickness fluctuation enhancement in the NSE signal occurs at the same *q*-value as the dip signifying membrane thickness in the SANS signal.

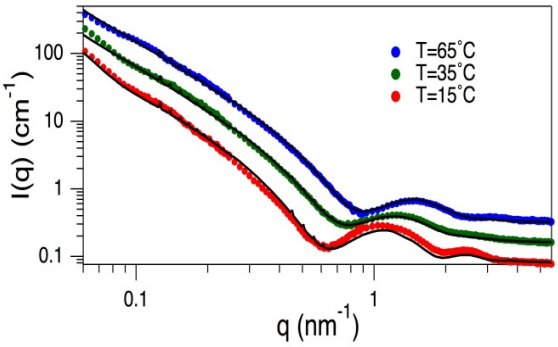

Fig. S4. SANS data from the tail-contrast-matched equimolar DMPC/DSPC unilamellar vesicles, shifted vertically for clarity. The solid lines are the fit results to a three-shell vesicle model.

1. Woodka AC, Butler PD, Porcar L, Farago B, & Nagao M (2012) Lipid Bilayers and Membrane Dynamics: Insight into Thickness Fluctuations. *Physical Review Letters* **109**(5):058102.
2. Zilman AG & Granek R (1996) Undulations and Dynamic Structure Factor of Membranes. *Physical Review Letters* **77**(23):4788-4791.
3. Watson MC & Brown Frank LH (2010) Interpreting Membrane Scattering Experiments at the Mesoscale: The Contribution of Dissipation within the Bilayer. *Biophysical Journal* **98**(6):L9-L11.
4. Lee J-H, *et al.* (2010) Thermal Fluctuation and Elasticity of Lipid Vesicles Interacting with Pore-Forming Peptides. *Physical Review Letters* **105**(3):038101.
5. Nagao M (2009) Observation of local thickness fluctuations in surfactant membranes using neutron spin echo. *Physical Review E* **80**(3):031606.
6. Nagao M, Chawang S, & Hawa T (2011) Interlayer distance dependence of thickness fluctuations in a swollen lamellar phase. *Soft Matter* **7**(14):6598-6605.
7. Nallet F, Laversanne R, & Roux D (1993) Modelling X-ray or neutron scattering spectra of lyotropic lamellar phases: interplay between form and structure factors. *Journal de Physique II* **3**(4):487-502.
8. Guinier A & Fournet G (1955) Small angle X-rays. (Wiley, New York).